

PRELIMINARY INVESTIGATIONS OF CREEP STRAIN OF NEOGENE CLAY FROM WARSAW IN DRAINED TRIAXIAL TESTS ASSISTED BY COMPUTED MICROTOMOGRAPHY

ŁUKASZ DOMINIK KACZMAREK, PAWEŁ JÓZEF DOBAK, KAMIL KIELBASIŃSKI

University of Warsaw, Faculty of Geology

Abstract: The study concerns soil creep deformation in multistage triaxial stress tests under drained conditions. High resolution X-ray computed microtomography (X μ CT) was involved in structure recognition before and after triaxial tests. Undisturbed Neogene clay samples, which are widespread in central Poland, were used in this study. X μ CT was used to identify representative sample series and informed the detection and rejection of unreliable ones. Maximum deviatoric stress for in situ stress confining condition was equal 95.1 kPa. This result helped in the design of further multistage investigations. The study identified the rheological strain course, which can be broken down into three characterizations: decreasing creep strain rate, transitional constant creep velocity, and accelerating creep deformation. The study found that due to multistage creep loading, the samples were strengthened. Furthermore, there is a visibly “brittle” character of failure, which may be the consequence of the microstructure transformation as a function of time as well as collapse of voids. Due to the glacial tectonic history of the analyzed samples, the reactivation of microcracks might also serve as an explanation. The number of the various sizes of shear planes after failure is confirmed by X μ CT overexposure.

Key words: *microstructure, multistage creep tests, strain rate, undisturbed Neogene clay*

1. INTRODUCTION

Investigating creep is fundamental for practical issues, such as assessing the stability of slopes of hills and embankments which are in a constant stress state. In order to recreate the real three-dimensional stress state and strain field, triaxial tests were applied in the present study.

The general definition of creep is the soil strain rate in a constant non-failure stress regime. The soil creep rate can vary with both time and stress level. Theories concerning creep genesis have been reviewed in [18]. Based on the SEM structure images [21] as well as preconsolidation of soil being analyzed (OCR \sim 4) and glacial tectonic history ([9], [22], [28], [36]) it seems that creep in samples under study is caused mainly by the breakdown of interparticle bonds, water flow from micropores to macropores as well as sliding between the soil particles, and deformation due to structural viscosity. The above has been described in detail in [23]. Some literature deals with case studies under drained and undrained conditions, using triaxial apparatus, with one-dimensional theories adjusted for three-dimensional stress states (e.g. [34], [39]). It has been reported in [37] that drained

creep time is longer than creep in undrained condition. In [24], it has been shown that under the same deviatoric stress, the axial strain of the undrained creep test is lower than in the drained creep test. This has been explained by the fact that, in an undrained triaxial creep test, deformation is generated only by creep; however, during the drained triaxial test, deformation is caused by both consolidation and creep.

The research question in this study concerns the course of strain changes in the drained condition during constant stress state resulting in creep soil strain. Therefore, several multistage (multistress levels) drained triaxial creep tests were performed as the preliminary investigations. Further the study is planned, concern creep strain under undrained conditions. In one test axial and radial strain measuring sensors were used to determine the full characteristics of soil behaviour during the triaxial tests. Neogene clay was used in the study, due to its prevalence at construction sites in Warsaw. In the case of undisturbed cohesive soil with strong involvement of glacial tectonic history ([21], [22]) we expect structure heterogeneity, microcracks and even empty voids. For non-invasive and non-destructive internal structure recognition, X-ray computed microtomography (X μ CT) was used.

2. MATERIAL

In this study, samples of undisturbed Neogene clay were used. The Neogene clay from Warsaw is a Neogene lacustrine deposit, which has been described in detail, e.g., in [3], [21], [30]. The samples used in this study came from the north-eastern part of the Miocene Basin (Fig. 1). As Fig. 1 shows, this soil type is com-

mon in large areas of Poland. More information can be found in [5], [9], [21], [22].

The glacial tectonic history of Neogene clay area affects macro visible layer folding and microstructure reconstruction (Fig. 2). The overconsolidated stress-strain behavior of the analyzed clay is the result of geological history: first, long-term slow sedimentation, then glacier overburden and finally unburden due to Vistula river erosion [28]. Due to this

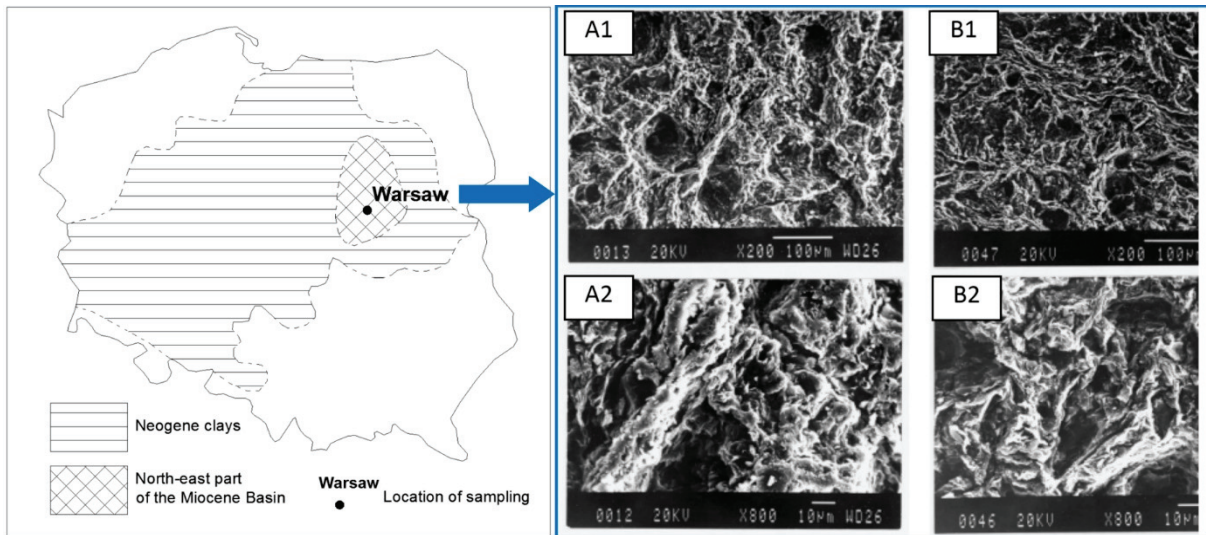


Fig. 1. Distribution of Neogene clay ([7] based on [35]); typical SEM micrographs of Neogene clay from Warsaw: A1,2 – sample with matrix-turbulent microstructure; B1,2 – sample with laminar-turbulent microstructure [20]

mon in large areas of Poland. The samples were cut from monoliths collected from excavation walls of “Copernicus Science Center” metro station. Samples were taken from the depth of 10 m below ground surface and 2 m below the Neogene clay layer top. The water table in this area is around 5 m below ground surface ([1], [17]).

In the case of this particular soil, the microstructure plays a great role in determining the stress-strain characteristics ([9], [20], [22]), which is important in terms of creep deformation ([23]). The microstructure, hence the distribution and connection of clay particles, of the soil is a type of mixed package containing mainly beidellite (smectite)-illite. Within the soil structure, there are well visible macropores and micropores (Fig. 1.A1,2; 1.B1,2) which can be involved in creep deformations. The microstructure of Neogene clay may be variable in the Warsaw area [20]. Neogene clay microstructure is partly determined by the sedimentation condition (e.g. microstructure of turbulent or laminar-turbulent; Fig. 1.A1,2; 1.B1,2) and by load history. The microstructure of Neogene clay from Warsaw is comparable with the microstructure

history Neogene clay is sensitive to moisture and structure changes [21]. Furthermore, in the scale of clay particles, there are microcracks that can cause brittle ruptures [21]. Discontinuity-cracking develops due to the brittle nature of destruction at a time when sediment was already relatively consolidated [21]. Microcracks are the privileged areas of failure surface formation ([9], [22]).

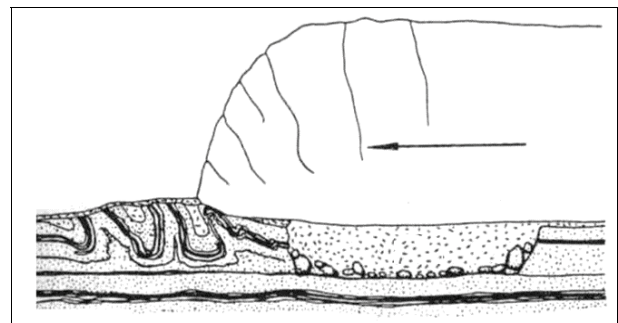


Fig. 2. Glacial tectonic mechanism; front of glacier folding [6]

During sample preparation, the variability of soil and even the presence of voids (Fig. 3) could be ob-

served. Moreover, there were visible fine discontinuities which visualized on the fresh cutting surfaces. In compliance with the standards [27] cylindrical samples with the height diameter slenderness = 2 and 3.6 cm in diameter were prepared for triaxial tests.



Fig. 3. Identification of the void inside (white arrow) the monolith during the preparation of samples

Table 1. Selected physical properties of Neogene clay under study

Physical properties	Results			
	Study samples of clay	Weathred clay [21]	Unweathered clay	
			[7], [3]	[26]
Moisture w_n (%)	31–22	30–45	16.7–40.2	16.6–35.6
Bulk density ρ (Mg/m ²)	1.91–1.94	1.7–2.0	1.85–2.17	1.86–2.11
Liquid limit LL (%)	76.6	up to 100	35.5–115.9	49.6–99.0
Plastic limit PL (%)	40	up to 40	16.8–49.8	18.0–43.6
Plasticity Index PI (%)	36.6	up to 60	16.9–72.9	31.6–66.7
Clay particle size < 0.002 mm	46	20–85	13–90	41–90

The basic physical properties of the Neogene clay were measured and the values were presented in [15] and [16]. The selected parameters are shown in Table 1 against the background of regional studies for Warsaw.

Based on the results, we can conclude that the parameters of the study material are in good agreement with results of previous analysis of Neogene clay from Warsaw. The obtained parameter values are between those of unweathered clay and weak wethread clay, which lies in the first few meters of Neogene clay in Warsaw [21].

3. METHODOLOGY

Having determined the physical parameters of soil, the next stage is to select representative samples series using X μ CT, which is crucial for the results. First, maximum deviatoric stress has to be defined. For this purpose, a standard triaxial test is performed. According to the Coulomb-Mohr failure criterion, the sample failure structure can also reveal information about strength mobilization [31]. The number of shear planes too can deliver information about structure changes, in terms of whether it is more brittle or ductile. The creep course study is shown schematically in the Fig. 4.

3.1. MICROTOMOGRAPHY OVEREXPOSURE

In the second and final stage X μ CT was used. This method is based on electron absorption through overexposure. The magnitude of absorption correlates to density. Hence, the higher density zones of the analyzed material enhance object recognition. There are three elementary stages of X μ CT tests: data acquisition, data registration and image processing. Figure 5 shows how material density information is converted into a X μ CT cross section. Further detailed information in relation to soil can be found in e.g. [13], [26].

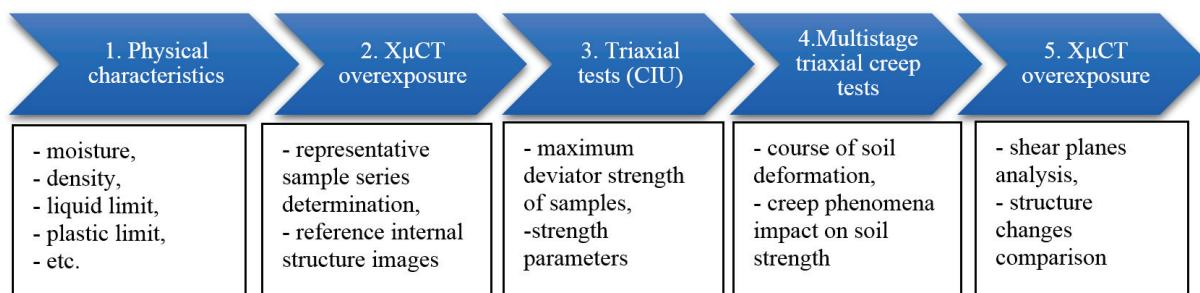


Fig. 4. Workflow of the creep deformation course study

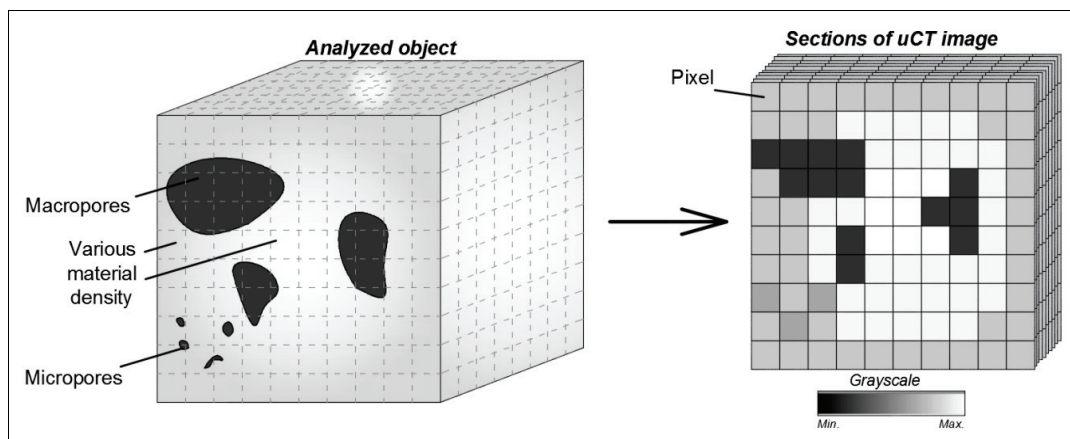


Fig. 5. Conversion of the various density zones in the analyzed object into a X μ CT cross section in grayscale

X μ CT possibilities of microstructure analysis of composite material were presented in [11]. Furthermore, grey value images generated by the X μ CT technique can serve as a basis for finite element models and following numerical simulations of, e.g., compression ([19], [32]). In the case of the analyzed Neogene clay, the pixel size was approximately 25 μ m. More information on X μ CT Neogene clay recognition has been published under papers [14] and [16].

3.2. TRIAXIAL TESTS (CIU)

The triaxial tests in the third stage were performed using the CIU (consolidated isotropically undrained) method. This method involves isotropical consolidation with shear compression in undrained conditions and pore pressure measurement. Short time duration was one of the reasons why this method was chosen for recognition of soil shear strength. It should be highlighted that the undrained strength parameters of Neogene clay from Warsaw are convergent with those determined under drained conditions [8]. For such a correlation, the requirements that must be met are full water saturation and consolidation [8]. In the further creep investigation, triaxial tests using the CID (consolidated isotropically drained) method were performed. In this method, prior to consolidation phase clay sample is subjected to water saturation through back pressure (Skempton's B-value for analyzed samples of this stage was in the range 75-87%). The procedures applied in the tests confirm to the requirements of [10], remarks contained therein and technical standards [27].

The maximum deviatoric stress (q_f) was determined based on CIU tests performed with constant shear compression velocity ($v_s = 0.01$ mm/min) and after consolidation, which restored various confining

pressure conditions (also in situ stress condition). In order to define the soil strength parameters, the triaxial tests sequence for three samples were determined. The sequence of effective confining pressures for triaxial tests (CIU) was:

- 100 kPa for sample 1T (cell pressure 1000 kPa, back pressure 900 kPa);
- 200 kPa for sample 2T (*in situ* stress; cell pressure 480 kPa, back pressure 280 kPa);
- 300 kPa for sample 3T (cell pressure 580 kPa, back pressure 280 kPa).

Initially, the triaxial CIU tests were designed with 280 kPa back pressure and 380, 480, 580 kPa cell pressure. First, samples 2T and 3T were tested under initially designed conditions. In these tests the consolidation took approximately two and a half weeks. Therefore, the following test of sample 1T was performed with higher pressure in order to shorten the consolidation time. In this case, the consolidation stage took around 3 days, and the B-value of water saturation was higher. Thus, further triaxial drained creep tests were performed under higher pressure.

3.3. MULTISTAGE TRIAXIAL CREEP TESTS

The fourth stage lies at the heart of the present study procedure. It concerns multistage creep tests in a triaxial stress state with drained conditions. Due to drained condition, the control of the effective axial stress is more convenient and accessible than in case of undrained condition, where the effective stress is changing in relation to pore pressure adjustment. Nevertheless, the creep investigation under undrained condition is next planned step, which will be analyzed in the near future and then published. During this stage, which is based on the results obtained in the previous third stage (determination of the maximum deviatoric

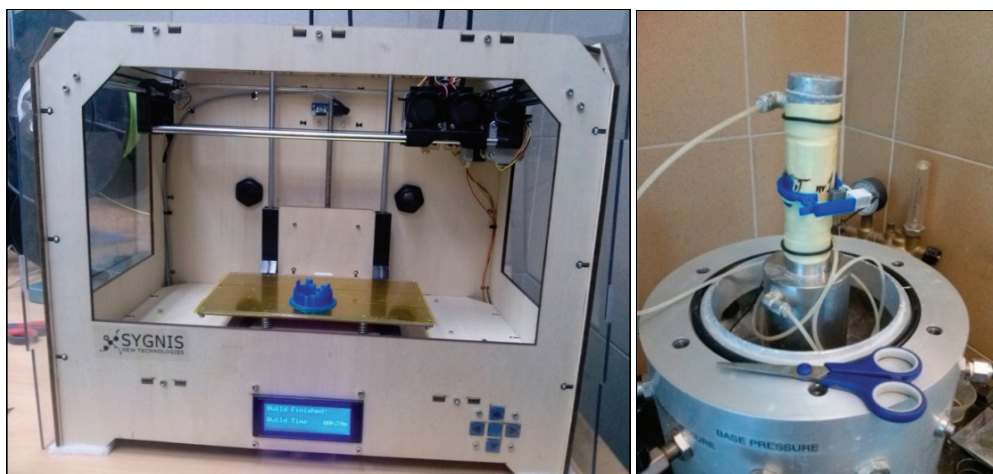


Fig. 6. Elements supporting the radial strain sensor designed specifically for the sample dimensions

Table 2. Program for Multistage Drained Triaxial Creep Tests in compression conditions ($\sigma' = 200$ kPa)

Test data		Stage No.								Comments
		1	2	3	4	5	6	7	8	
q [kPa]		42.80	57.06	80.84	95.10	109.37	123.63	137.90	152.16	
SL*		0.45	0.60	0.85	1.00	1.15	1.30	1.45	1.60	
Sample 1a	t [days]	20		15						Apparatus malfunction
Sample 1b		6	2	4	5	4.5	1	~0.5		With radial strain sensor
Sample 2			10	10	10	10	10	10	~0	
Sample 3				10	10	10	10	~0.5		

* Stress level $SL = q/q_r [-]$.

stress), four multistage triaxial tests with different fixed deviatoric stress levels (SL) and with consolidation at the *in situ* stress condition were designed (Table 2) for triggering creep strains. Clay sample water saturation was performed with the back pressure procedure (Skempton’s B-value for analyzed samples in this stage was in the range 88–93%). At this stage, sample 1a was in a compression state with cell pressure of 480 kPa and pore pressure of 280 kPa. Samples 1b, 2, 3 were in a compression state with cell pressure of 1000 kPa and pore pressure of 800 kPa. In both configurations, the effective confining pressure was equal: 200 kPa (*in situ* stress condition) and in both cases after consolidation, deviatoric stress was applied instantly and held constant for a period of time in order for the creep to occur. Then deviatoric stress was increased to initiate the next creep stage, and so on, until failure occurred. Multistage creep means that one sample can be used to conduct more than one stage of creep testing. During creep testing, the creep load is automatically revised to keep deviatoric stress constant ($q_f = \sigma_1 - \sigma_2$). In order to analyze the complete behavior of Neogene clay from Warsaw,

the specific direct radial strain sensor (based on the Hall effect) holders were designed and printed off with a 3-D printer for a specific sample size (Fig. 6). The radial strain sensor were used during 1b triaxial creep test.

4. RESULTS AND DISCUSSION

X μ CT results are shown in Tables 3–5, 7, and 8. Thanks to use of X μ CT method the samples with interrupt of structure, like voids or fractures (Table 3), were identified and rejected. Furthermore, the geometry of sample 01 shows extensive relief, which was revealed because of density differences. Table 4 presents examples of reliable samples, which were chosen for further triaxial (CIU) investigation. The structure is heterogeneous, nevertheless, there are no privilege zones for failure beginning. This is important for the accuracy of result in the soil strength test, especially in the case where the results are used in designed of further triaxial creep tests. Table 5 shows the results

Table 3. X μ CT sample recognition – rejected samples (white arrows indicate structure interruption)

Sample No.	X μ CT cross-sections	X μ CT sample geometry
01		
02		

Table 4. X μ CT recognition examples of selected samples prior to triaxial tests (CIU)

Sample No.	X μ CT cross-sections	X μ CT sample geometry
2T		
3T		

Table 5. Selected X μ CT sample cross-sections after triaxial tests (CIU) with presumptive shear planes (white lines) and stress field (red and orange arrows)

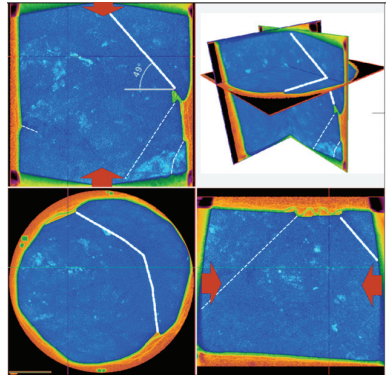
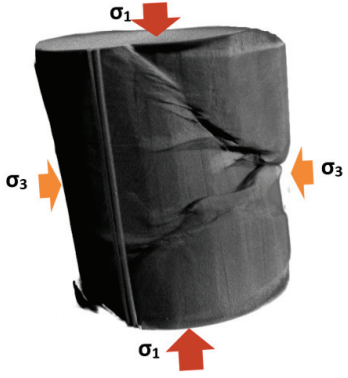
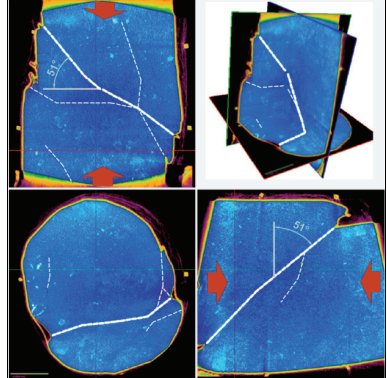
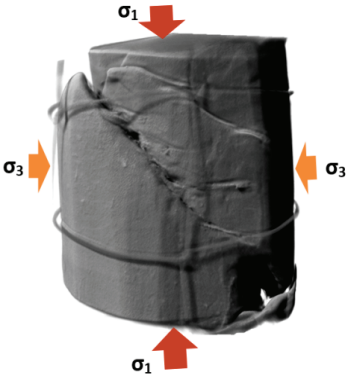
Sample No.	X μ CT cross-sections	X μ CT sample geometry
2T		
3T		

Table 6. Maximum deviatoric stress determined by means of triaxial tests (CIU)

Sample	Effective Confining pressure (cell pressure, pore water pressure) σ' [kPa]	Maximum deviatoric stress q_f [kPa]	Angle of shear plane (major plane) θ [°]
1T	100 (1000, 900)	86.0	42–66 (50)
2T	200* (480, 280)	95.1	49–57 (49)
3T	300 (580, 280)	117.3	43–51 (51)

* in situ stress condition.

of triaxial tests. Each of this tests ended by shear plane growth. [31] in their study pointed out the relation between shear plane angle and maximum soil strength mobilization, which was not disturbed by any privilege zone of destruction, based on Coulomb-Mohr failure criterion. According to this study, one of the indications of intact soil failure is greater shear plane angle than 45 degrees ($\theta = 45^\circ + \varphi'/2$). We can see in Table 6 that this requirement has been satisfied, and so, the results can be used for further investigation procedures.

Table 6 and Fig. 7 give a brief account of the results of triaxial (CIU) tests. The maximum deviatoric stress, for sample 2T under *in situ* stress conditions, is

95.1 kPa. With the confining pressure being 100 kPa less, the deviatoric stress is appropriately 10% lower. In the opposite case of the effective confining pressure being 100 kPa higher, the deviatoric stress increase to approximately 20%. Based on these results, the cohesion and the internal friction angle were calculated ($c' = 25$ kPa; $\varphi' = 7^\circ$). For comparison, a review paper [21] indicated the range of c' (25–55 kPa) and φ' (12–22°) for unweathered Neogene clay from the Warsaw area and the range of c' (up to 10–25 kPa) and φ' (up to 10–13°) for the weathered one. Furthermore, the data of soil strength was gathered by [21]: for unweathered soil it is 8–250 kPa, and for weathered one it is up to 80 kPa. The geological history was

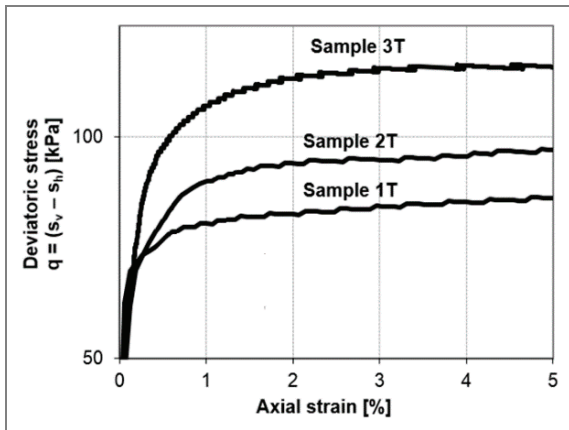


Fig. 7. Relation between deviatoric stress versus axial strain in triaxial tests (CIU)

also pointed to in [21] as the crucial factor for Neogene clay strength, especially for the upper part of the soil layer.

Analyzing the strength parameters obtained against the results presented in [21], it can be stated that the cohesion value is somewhere between those typical of weathered and unweathered Neogene clays. The internal angle of friction is in the range of parameters of weathered soil. However, it is noteworthy that the calculated values of parameters could also be affected by swelling phenomena. During the saturation of the samples in triaxial apparatus the swelling pressure was taken into account (earlier studies have shown approximately 45 kPa of swelling pressure). Nevertheless it has been pointed out in [21] that the swelling

Table 7. Representative samples series dedicated for triaxial creep tests distinguished by X μ CT recognition

Sample No.	X μ CT cross-sections	X μ CT sample geometry
1b		
2		
3		

pressure in Neogene clay taken from Warsaw area is between 20 and 280 kPa. In the event of the swelling pressure being higher than assumed, the strength parameters could be reduced (especially the internal friction angle). This issue will be subject to further verification in the next study.

Table 7 shows the internal structure of solid soil samples which are comparable to each other as well as to previous samples (used in triaxial CIU tests). These three samples are dedicated to further multistage triaxial creep tests. Various shades (from light blue to dark blue) indicate the density of the material. The lighter material color is correlated to the more dense area.

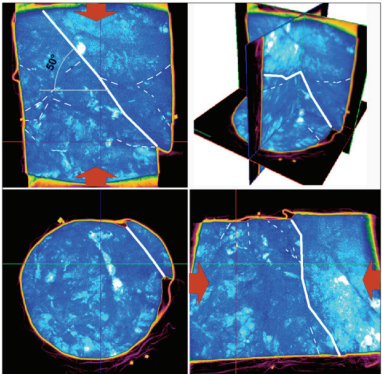
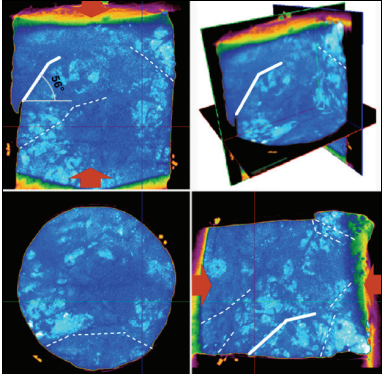
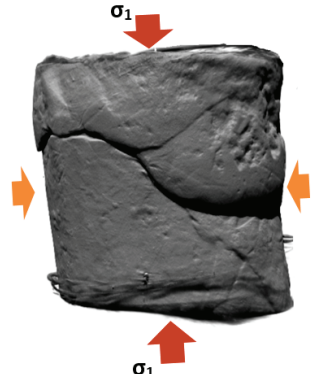
Table 8 shows the example of the X μ CT recognition of the sample after multistage triaxial creep test, which ended in failure and shear plane growth. In contrast to the results of the standard triaxial (CIU) tests, in the case of creep tests, there is one major shear plane with finer microcracks. Such an effect can be related to the progressive loading and thus stiffen the structure of the sample clay particle. Therefore, more brittle destruction occurred. The presence and the number of fine microcracks can be compounded by reactivation of old discontinuities. What is more, we do not observed a shear plane of less than 45 degrees, which means that the final failure occurs during

maximum deviatoric stress. Hence, we can assume that during the test, before the failure at maximum deviatoric stress, the reactivations of old discontinuities have occurred and stopped at some lower deviatoric stress. This may be the reason of the visible changes in the deformation velocity.

The very essence of this paper is presented in Figs. 9 through 12. They show the results of multistage triaxial creep tests (Table 2), represented by the axial strain vs. time curves and provide a summary of strain rate calculations (Table 9). Strain rate values are treated here as comparable magnitudes indicating the course of creep deformation. The sample 1b test, a radial sensor was involved during data acquisition. The radial curve of this test mimics axial strain curve but there are some differences. For instance, there is no radial strain and, at the same time, axial strain progresses in the first stress level (SL = 0.45) when testing sample 1b. Such behavior can be the effect of microstructure densification and thereby increase of soil strength.

The linearity of strain-time curves is disturbed by load applications with use of rigid stem as well as by stepwise jumps of strain curves. In order to obtain a more unequivocal curve in case of load application effect in the very beginning, the register strain jumps in the first stages of all the tests were cut

Table 8. Selected X μ CT recognition of sample 1b and 2 after multistage triaxial creep tests with presumptive shear planes (white lines) and stress field (red and orange arrows)

Sample No.	X μ CT cross-sections	X μ CT sample geometry
1b		
2		

off. In sample 1a, 2.72% strain increase was deleted within first seconds of the first stage. In sample 1b, 1.33% was deleted. In the case of sample 2, 0.99% was removed and in sample 3, 0.95% was abolished. For simplicity of curve slope (i.e., strain rate) calculations, further data processing was performed. In the case of samples where strain jumps were observed (sample 1a, 1b, and 2), all these jumps were cut off for trend analysis. Consequently, we obtained two curves; the first called “rough data” and the second called “clear data”. An example of “rough data” curves are presented in this paper (Figs. 9A and 10.A). Detailed analyses of data acquisition with a 1s step revealed temporary fluctuation of axial load during long-term nonstandard tests. They are the result of a not fully adapted control system to creep tests. In literature, close cases of the control system impact on the results of compression tests can be found. In [25]

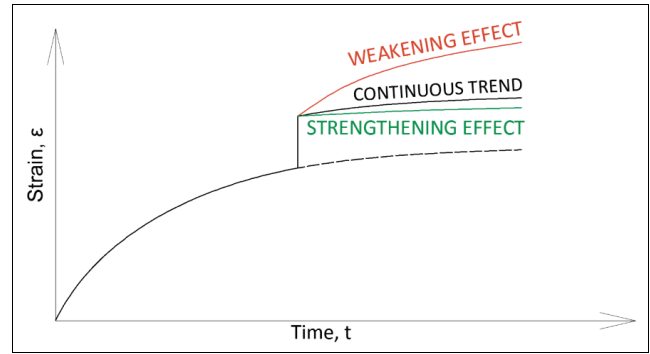


Fig. 8. Scheme of temporary fluctuation of axial load during long-term tests assessment on the structure of soil by strain rate analysis

control and measurement system, based on double feedback loop, is indicated as important component of result quality improvement. In the analyzed creep tests

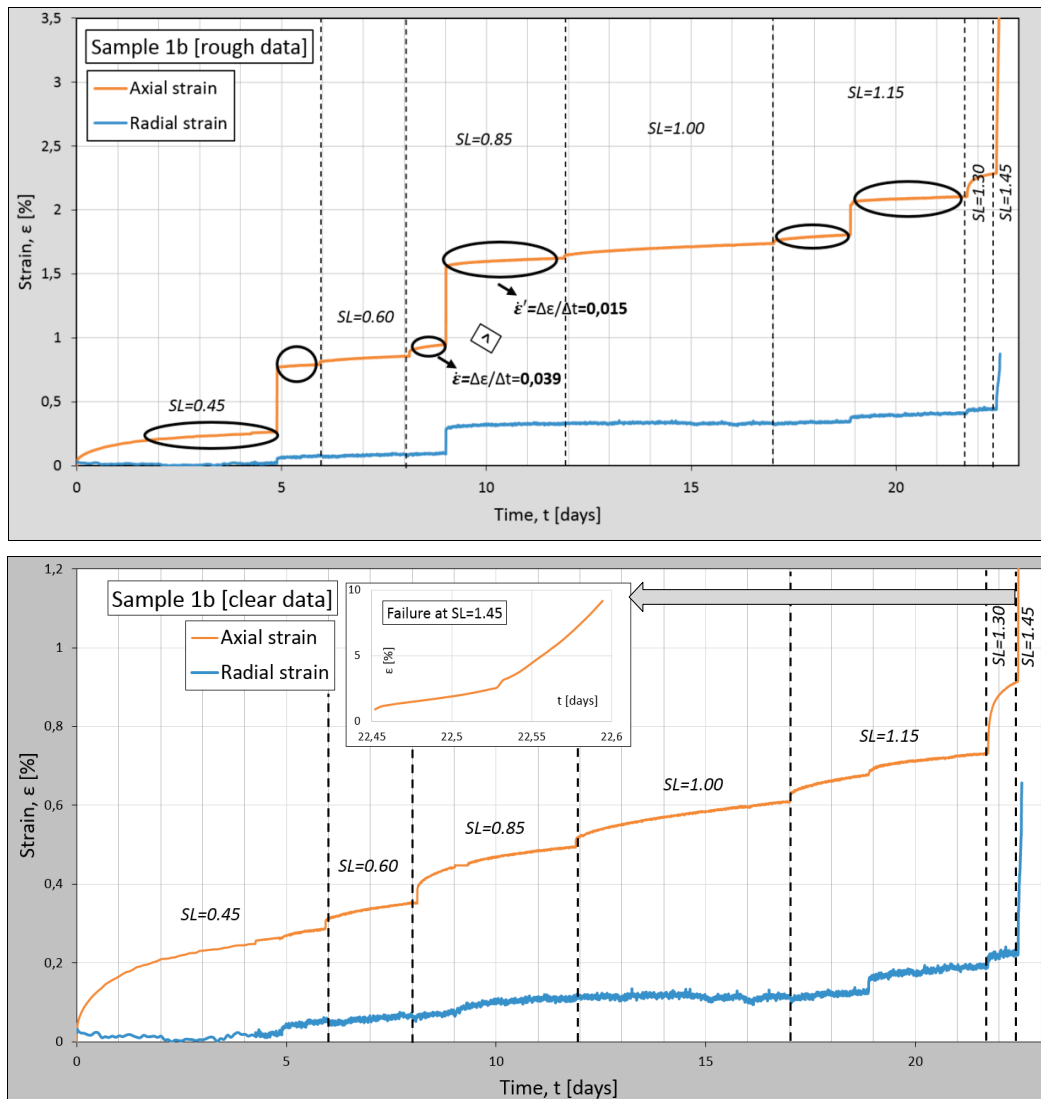


Fig. 9. The result of the multistage triaxial creep test of sample 1b: A – rough data with indicated example of strain rate analysis; B – data after processing

outcomes, only in the last failure phase of long-term creep tests observed strain jumps are related to structural damage such as void collapses and old fine microcrack reactivations. Due to a technical issue the effect of load changes should be assessed. To achieve this, strain rate analyses were performed. The strain rates before and after observed stepwise shifts were calculated and amalgamated in Table 9. These values were used for quantity comparison of stepwise shift influence on soil structure. Figure 8 shows a scheme of stepwise strain shift interpretations.

During the data processing, the changes of the strains dynamics were kept. They can be observed in Fig. 10 (sample 2) and Fig. 11 (sample 3) at 1.45 stress level and 1.15 stress level respectively. There are firstly decreasing strain rate, then some period of linear stable strain value, and once again slowly accelerating strain rate. That behavior could be explained by microstructure transformation and so stress field redistribution inside the samples.

According to Figs. 9–11 three general creep dynamics characteristics can be distinguished: with in-

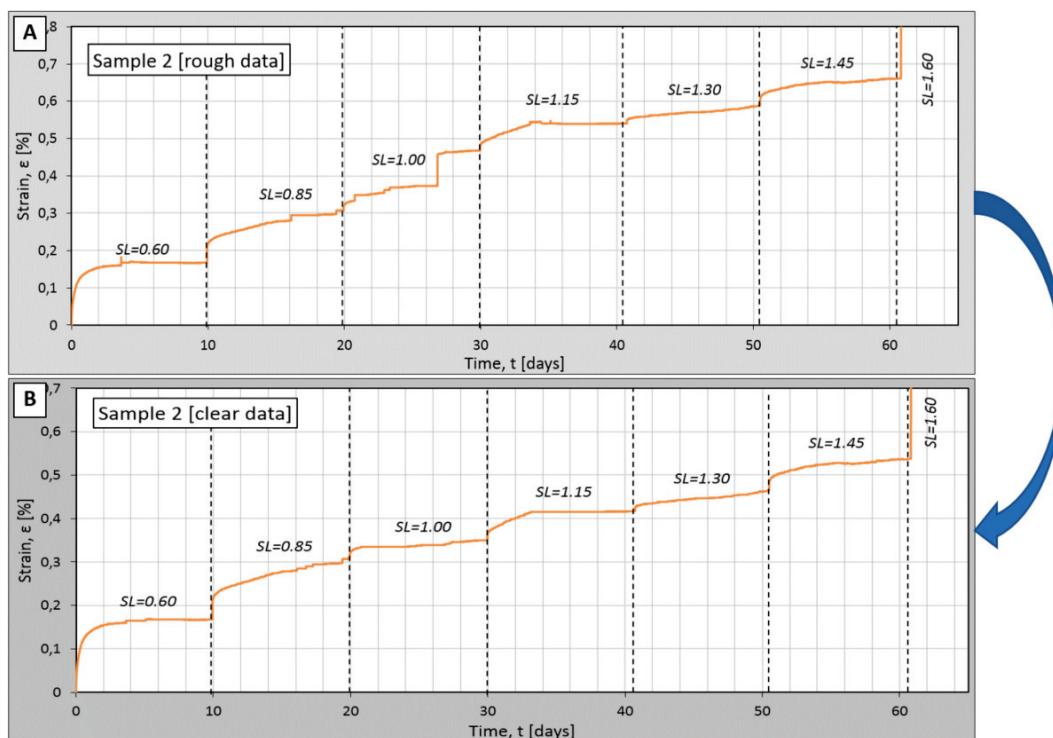


Fig. 10. The result of the multistage triaxial creep test of sample 2: A – rough data; B – data after processing

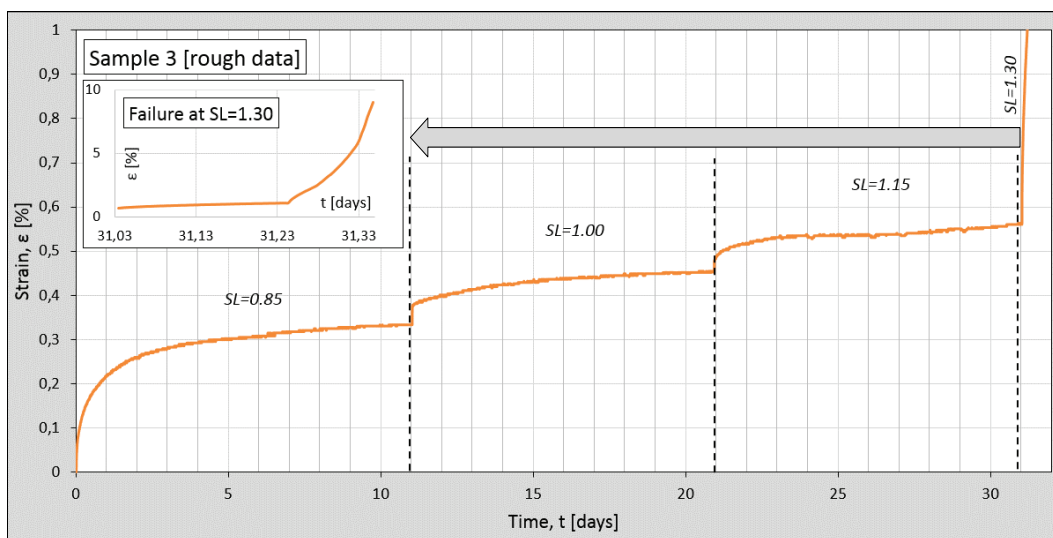


Fig. 11. The result of the multistage triaxial creep test of sample 3: A – rough data; B – data after processing

creasing strain rate, constant value of deformation, and with decreasing speed of deformation. The change of strain rate is similar during the various creep deformation stages up to the stage before the failure, followed by an apparent increase. In the last failure stage, which is correlated with much higher stress level than maximum deviatoric stress, we can observe the brittle behavior of soil structure during plastic flow. Specifically, strain rate is jumping up but then something (probable structure friction) is slowing it down and so on again. Furthermore, the creep stage with increasing strain rate until failure can be broken down into three phases (Fig. 12): transitional, stable and accelerating followed by failure moment. In sample 3 test the accelerating phase is so rapid that it is hard to distinguish. Similar three phase characteristics were observed in [24] during marine Hong Kong clay tests.

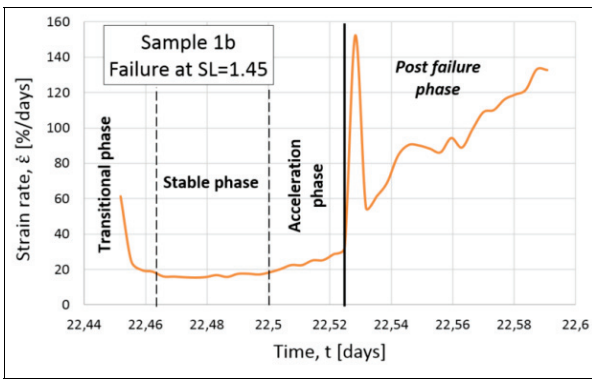


Fig. 12. Part of curve representing accelerating creep strain rate within characteristic phases distinguished for sample 1b

In the case of sample 2 multistage creep test, at 1.60 SL stage, there was the unplanned increase of compression load and in consequence the failure of the sample. At least, from data registration, we could recover the maximum deviatoric stress during failure. It was much higher than planned 152.16 kPa (approximately 210 kPa). Obviously, the instantaneous strength of soil is higher than long-term strength. Nevertheless, the slope of the strain-time curve presents a similar tendency to other tests.

Various strain rate dynamics have few explaining hypotheses: (i) structural voids collapses, (ii) old microcracks reactivations in the scale of clay particles ([21], [22]), all together. The observed creep dynamics characteristics are forced by load magnitude. [38] has proposed the following explanation of attenuating and accelerating strain rate kinematic: in the event of low load magnitude the soil structure has some defects but, simultaneously, new bonds are formed. Such effect combined with the closely packed particle arrangement produce a “healing” effect for soil structure. In other words, we observed hardening phenomena, which produces soil volume shrinking and soil structure strengthening. In the opposite case, under a sufficiently high load, the structure weakens as the creep progresses [38]. This is because breaking of bonds, particle reorientations, void collapse and further structural damage prevent the “healing” effect. Strain rate accelerates until the structural damage reaches a critical state and the failure occurs. Figure 13 illustrates the described mechanism.

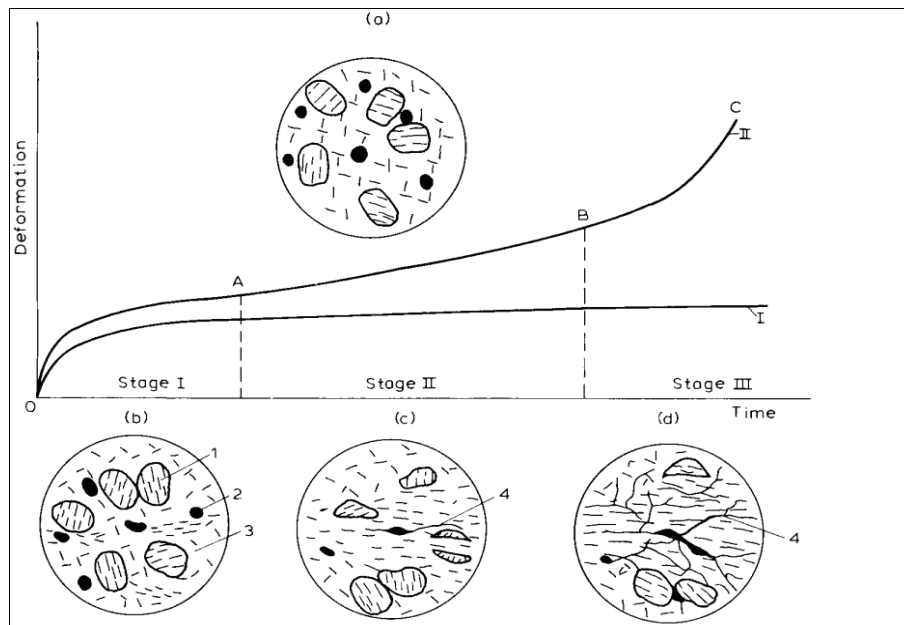


Fig. 13. Schematic representation of changes in microstructure of soil due to creep: (a) initial structure; (b) structure at stage I; (c) structure at stage II; (d) structure at stage III of creep; 1 – micro-aggregates of clay particles; 2 – cavities and voids; 3 – cementing clay; 4 – micro- and macro-cracks [33]

Table 9. Strain rate results for Multistage Drained Triaxial Creep Tests

Sample		Stress level								Comments	
$X_{\mu CT}$											
before	after	0.45	0.60	0.85	1.00	1.15	1.30	1.45	1.60		
1a		0.01/~0/~0	–	0.02/0.01	–	–	–	–	–	Apparatus malfunction	
1b		0.01/0.01	0.02	0.04/0.02	0.02	0.02/0.01	0.09	18/102 (F)	–	Axial	Strain
		~0/~0	0.01	0.01/0.01	~0	0.01/0.01	0.04	11 (F)	–	Radial	
2		–	~0	0.01/0	0.01/~0/0	0.02/~0	0.01	0.01 → ~0	(F)		
3		–	–	0.01	~0	0.01	2/70 (F)	–	–		

/ – microcracks or external interference,
 → – change into,
 (F) – failure,
 Mean value of measurement accuracy: 0.005.

Table 9 gives a summary of all calculated curve slopes (i.e., strain rates) of the triaxial creep tests. Slopes were calculated as the ratio of strain [%] changes and period of time [days] needed for this.

In the table, there are various symbols, which helps in the reflection of calculation sequence. For instance, during the strain jump (the symbol of which is “/”), the slope before and after is calculated. During these calculations, the slope at the beginning of each stage, when the load is applied, is higher than latter and it is not considered. In the present study, the creep deformation is considered, therefore strain rates without the impact of the immediate elastic answer for stem influence.

The multistage creep tests were started each time from higher stress level. Thanks to that we can treat the first stages of each tests as one stage test. When we comprise in such manner the strain curve slopes for the same stress levels (not triggering failure) but different tests we can observe little change in case of analyzed overconsolidated Neogen clay.

Having analyzed strain rates before and after axial load fluctuations, which generated strain shifts, it can be concluded that the structure of soil samples 1a, 1b and 2 and were compacted. Hence, the samples have been strengthened. In sample 3, where no jumps was observed, the strength was greater than that determined by the CIU test but less by about 15% compared to the creep triaxial tests where jumps were observed. With test number increase, the results will be verified. To use the results for further deformation predictions, the strain rates before the strain jumps should be employed.

The nature of observed strains may be approximated by numerous rheologic models. Rheological

models can be implemented into numerical simulations in order to forecast magnitude of displacements based on various data, such as laboratory tests results, geodetic monitoring, etc. (e.g., [29], [38]). One of the composed, universal model taking into consideration the combination a few of the based elements was proposed in [4]. It can described as the rheological function R in a structural form:

$$R = T_f(H - K - Z - P_r)$$

where:

T_f - Terzaghi's hydrodynamic model,

H – the model of ideal, elastic Hooke's body,

K – the model of Kelvin's body (corresponding to viscoelastic strains),

Z – proposed body contained Prandtl's and St. Venant's elements and the wedge between lateral planes; their contact is described by plasticity modulus (this part of model is corresponding to plastic strain),

P_r – model of solid Prandtl's body (corresponding to plasticity flow).

This compound model is meant to explain, among other things, strain ε – time t relations, which would lead to stabilization of strain or constant velocity of strain. This second case involves excess of load capacity value Q and thereby, activation of St. Venant's element. The cutoff value for linear and straight part of $\varepsilon - t$ curve is fixed by t_{kr} . The initial part of strain depends on elements H and Z . A further part of curve line is correlated with element K and is a function of seepage process, too. The slope of advanced straight line $\varepsilon - t$ should be connected with nature of element Z .

Additionally, experimental data of analyzed tests shows oversteps of theoretical behavior sometimes.

This can be described by non-reversible horizontal displacements. Physically it reflects the friction during displacements of soil particles or part of the sample's body alike in analyzed, experimental tests.

6. SUMMARY

In this study, a series of tests were performed to analyze the character of creep deformation of undisturbed Neogene clay in Warsaw area. The study started in structure recognition and determination of representative soil samples by the X-ray computed microtomography (X μ CT). Then, standard triaxial tests (CIU) were performed in order to obtain maximum deviatoric stress in various confining conditions as well as to determine the strength parameter (cohesion, internal friction angle). Due to these results further multistage consolidated-drained triaxial creep tests were designed and carried out under various stress levels. Finally, subsequently to all triaxial tests, the X μ CT was employed to structure changes.

The obtained results are the first part of complete recognition of creep strain behavior of Neogene clay. Therefore, they can be treated as premises to certain assumptions and as the directions for further tests. From this study the following conclusions can be drawn:

- There are three general creep course deformation characteristics: with increasing strain rate, constant value of deformation, and with decreasing speed of deformation. The creep with increasing strain rate until failure can be broken down into three phases: transitional, stable and accelerating with following failure moment.
- The change of rate strain is similar during the various creep deformation stages up to the stage before the failure, followed by an apparent increase.
- At the destructive stress level after the accelerating creep, the plastic flow occurs. It is worth noting that during the plastic flow the structure impact is observed in the form of abrupt changes of strain rate.
- Under multistage constant creep stress level started below maximum deviatoric stress of the tested sample in the *in situ* stress state, Neogene clay samples strengthen in function of time.
- The samples under multistage creep stress condition started from 0.45 and 0.60 maximum deviatoric stress obtained higher strength than the sample under multistage creep stress condition started from 0.85 deviatoric stress.
- The multistage creep tests were started each time from higher stress level. Thanks to that we can treat the first stages of each test as one-staged tests. When we comprise in such manner the strain curve slopes for the same stress levels (not triggering failure) but different tests we can observe little change in case of analyzed overconsolidated Neogene clay.
- In the case of analyzed sample 1b, the radial strain curve mimics the axial strain curve, although significantly lower values of radial strain were obtained, what is related to drained conditions. The acquisition of the radial strain makes it possible to calculate the volumetric strain.
- X μ CT has proved that it is useful for shear planes analysis as well as microcracks identification and for selection of representative samples series. Furthermore, this method enables for calculation of shear plane angle which is strongly correlated with strength characteristic of the sample (especially, with internal friction angle).
- Tested soil samples are typical for Neogene clay in Warsaw area. The strength parameters are from the lower range of unweathered clay, what can be correlated with: (i) the sample collection (upper part of clay layer) and so due to unburden of soil structure, (ii) its direct contact with groundwater, (iii) the reactivation of microcracks related to the geological history.

REFERENCES

- [1] BAJDA M., FALKOWSKI T., *Geotechnical tests for estimation of geological conditions of the escarpment zone of "Skarpa Warszawska" in the vicinity of Tamka Street*, Landform Analysis, 2014, 26, 77–84.
- [2] BARAŃSKI M., KACZYŃSKI R., BOROWCZYK M., KRAUŻLIŚ K., TRZCIŃSKI J., WÓJCIK E., ZAWRZYKRAJ P., *Ocena zachowania się ilów plioceńskich ze Stegien w warunkach naprężeń efektywnych*, Projekt badawczy KBN Nr 5 T12B 041 22, Archiwum NCN, Warszawa 2004.
- [3] BARAŃSKI M., WÓJCIK E., *Estimation of ability to volume changes of Mio-Pliocene clay from Warsaw*, Geologija, 2008, 50, 49–54.
- [4] BRZOSKO Z., *Nowy reologiczny model gruntów*. Biuletyn Geologiczny, t. 11, Wydawnictwa Uniwersytetu Warszawskiego, Warszawa 1969.
- [5] COSTA FILHO L.M., *A laboratory investigation of the undrained small strain behaviour of London clay. Geotechnical aspects of stiff and hard clays*, Geotechnical Special Publication, 1986, 2, 28–43.
- [6] DADLEZ R., JAROSZEWSKI W., *Tektonika*, PWN, Warsaw, Poland, 1994.
- [7] GAWRIUCZENKOW I., WÓJCIK E., *Comparison of expansive properties of Neogene clays from the Mazovia region*, Przegląd Geologiczny, 2003, 61(4), 243–247.

- [8] GODLEWSKI T., KACPRZAK G., WITOWSKI M., *Practical estimation of geotechnical parameters for the diaphragm wall design founded on Warsaw "pliocene" clays*, Civil and Environmental Engineering, 2013, 4(1), 13–19.
- [9] GORĄCZKO A., KUMOR M.K., *Pęcznienie mio-plioceńskich ilów serii poznańskiej z rejonu Bydgoszczy na tle ich litologii*, Biuletyn PIG, 2011, 446, 305–314.
- [10] HEAD K.H., *Manual of Soil Laboratory Testing*, Vol. 3. *Effective Stress Tests*, Pentech Press, London 1986.
- [11] RAJZAKOWSKA M., STEFANIUK D., ŁYDŻBA D., *Microstructure characterization by means of X-ray micro-CT and nanoindentation measurements*, Studia Geotechnica et Mechanica, 2015, 37(1), 75–84.
- [12] IZDEBSKA-MUCHA D., WÓJCİK E., *Evaluation of expansivity of Neogene clays and glacial tills from central Poland on the basis of suction tests*, Geological Quarterly, 2015, 59(3), 593–602.
- [13] JASTRZĘBSKA M., KALINOWSKA-PASIEKA M., *Wybrane metody badawcze we współczesnym laboratorium geotechnicznym: od podłoża do parametrów gruntowych*, Wydawnictwo Politechniki Śląskiej, Gliwice, Poland 2015.
- [14] KACZMAREK Ł., *Możliwości wykorzystania wysokorozdzielczej mikrotomografii komputerowej w badaniach geologiczno-inżynierskich na przykładzie analizy ilów mio-plioceńskich*, Przegląd Geologiczny, 2016, 64(2), 105–102.
- [15] KACZMAREK Ł., GAWRIUCZENKOW I., *Porównanie wyników różnych analiz zawartości substancji organicznej w ilach miopliocenijskich z podłoża stacji Centrum Nauki Kopernik II linii metra w Warszawie*, Przegląd Geologiczny, 2016, 64(7), 489–494.
- [16] KACZMAREK Ł., KIELBASIŃSKI K., *Propozycja wykorzystania wysokorozdzielczej mikrotomografii komputerowej do analizy gruntu spoistego w badaniach pełzania*, Prz. Nauk. Inż. Kszt. Środ., 2016, 25(3), 277–289.
- [17] KACZMAREK Ł., POPIELSKI P., *Numerical analysis of the impact of construction of an underground metro line on the urban environment – a case study from the Vistula Valley in Warsaw*, Przegląd Geologiczny, 2016, 64(4), 219–229.
- [18] KACZMAREK Ł., DOBAK P., *Overview of soil creep phenomenon*, Contemporary Trends in Geoscience, 2017, 6(1), 28–40, DOI: 10.1515/ctg-2017-0003.
- [19] KACZMAREK Ł., ZHAO Y., KONIETZKY H., WEJRZANOWSKI T., MAKSIMCZUK M., *Numerical approach in recognition of selected features of rock structure from hybrid hydrocarbon reservoir samples based on microtomography*, Studia Geotechnica et Mechanica, 2017, in press.
- [20] KACZYŃSKI R., *Overconsolidation and microstructures in Neogene clays from the Warsaw area*, Geological Quarterly, 2003, 47(1), 43–54.
- [21] KACZYŃSKI R., *Engineering geological behaviour of London and Warsaw clays*, Geologos, 2007, 11, 481–490.
- [22] KUMOR M.K., *Zmiany wytrzymałości i struktury iltu plioceńskiego pod wpływem zamrażania*, Arch. Hydrotech., 1985, 32, 461–473.
- [23] LE T.M., FATAHI B., KHABBAZ H., *Viscous Behaviour of Soft Clay and Inducing Factors*, Geotechnical and Geological Engineering, 2012, 30(5), 1069–1083, DOI: 10.1007/s10706-012-9535-0.
- [24] LUO Q., CHEN X., 2014, *Experimental Research on Creep Characteristics of Nansha Soft Soil*, The Scientific World Journal, 2012, 5, Article ID 968738, 8 pp., DOI: 10.1155/2014/968738.
- [25] NOWAKOWSKI A., RAK P., *Adaptacyjna kontrola parametrów pętli sprzężenia zwrotnego i jej zastosowanie do sterowania maszyn wytrzymałościowych*, [in:] 22 Zimowa Szkoła Mechaniki Górniczej, Karpacz, Poland, 15–19 March 1999, 211–220.
- [26] PIRES L.F., CÁSSARO F.A.M., Bacchi, O.O.S., REICHARDT K., *Gamma-Ray Computed Tomography in Soil Science: Some Applications*, [in:] L. Saba (Ed.), *Computed Tomography – Special Applications*, InTech, Rijeka, Croatia, 2011, 293–318.
- [27] PKN-CEN ISO/TS 17892-9:2009. *Badania geotechniczne. Badania laboratoryjne gruntów. Cz. 9: Badanie gruntów w aparacie trójosiowego ściskania po nasyceniu wodą*.
- [28] SARNACKA Z., *Stratygrafia osadów czwartorzędowych Warszawy i okolic*, Prace Państwowego Instytutu Geologicznego CXXXVII, Warszawa 1992.
- [29] SEGALINI A., GIANI G.P., FERRERO A.M., *Geomechanical studies on slow slope movements in Parma Apennine*, Engineering Geology, 2009, 109(1), 31–44, DOI: 10.1016/j.enggeo.2008.11.003.
- [30] SUPERCZYŃSKA M., *Wartość parametrów sprężystości w zakresie małych i średnich odkształceń ilów formacji poznańskiej z Warszawy*, Inżynieria Morska i Geotechnika, 2015, 3, 207–211.
- [31] STEFANIUK D., TANKIEWICZ M., STRÓŻYK J., *X-ray microtomography (μ CT) as a useful tool for visualization and interpretation of shear strength test results*, Studia Geotechnica et Mechanica, 2014, 36(4), 47–55.
- [32] SZLAZAK K., JAROSZEWICZ J., IDASZEK J., DEJACO A., HASSLINGER P., VASS V., HELLMICH C., SWIESZKOWSKI W., *Grey value images as a basis for finite element models and their mechanical properties*, [in:] *Bruker Micro-CT User Meeting, Abstract book*, Luxemburg, 9–12 May 2016, 145–149.
- [33] VYALOV S., *Rheological Fundamentals of Soil Mechanics*. Elsevier, Amsterdam, The Netherlands, 1986.
- [34] WANG Y.F., ZHOU Z.G., CAI Z.Y., *Studies about Creep Characteristic of Silty Clay on Triaxial Drained Creep Test*, Advances in Civil and Industrial Engineering, IV(580), 2014, 355–358, DOI: 10.4028/www.scientific.net/AMM.580-583.355.
- [35] WICHROWSKI Z., *Studium mineralogiczne ilów serii poznańskiej*, Arch. Min., 1981, 37, 93–195.
- [36] WYSOKIŃSKI L., *Kryterium dynamiki zbroczy na przykładzie badań brzegów zbiornika Włocławek*, Habilitation thesis, University of Warsaw, Warsaw, Poland, 1976.
- [37] YE Y., ZHANG Q., CAI D., CHEN F., YAO J., WANG L., *Study on New Method of Accelerated Clay Creep Characteristics Test*, [in:] 18th Int. Conf. on Soil Mechanics and Geot. Eng., Paris, France, 1–2 February, 2013, 461–464.
- [38] ZABUSKI L., *Prediction of the slope movements on the base of inclinometric measurements and numerical calculations*, Polish Geological Institute Special Papers, 2004, 15, 29–37.
- [39] ZHU J., ZHAO Y., YIN J., *Undrained Creep Behavior of a Silty Clay in Triaxial Tests*, Instrumentation, Testing, and Modeling of Soil and Rock Behavior, 2011, 222, 139–146, DOI: 10.1061/47633(412)19.